Global NEST Journal, Vol 19, No 3, pp 464-478

Batch and fixed-bed column studies for the biosorption of Cu(II) and Pb(II) by raw and treated date palm leaves and orange peel

Amin M.T.[1,2,] *, Alazba A.A.[1,3] and Shafiq M.[1]
[1]Alamoudi Water Research Chair, King Saud University, P. O. Box 2460, Riyadh 11451, Kingdom of Saudi Arabia
[2]Department of Environmental Sciences, COMSATS Institute of Information Technology, Abbottabad, 22060, Pakistan
[3] Agricultural Engineering Department, King Saud University, P. O. Box 2460, Riyadh 11451, Kingdom of Saudi Arabia
Received: 09/03/2017, Accepted: 25/08/2017, Available online: 22/10/2017
*to whom all correspondence should be addressed: e-mail: mtamin@ksu.edu.sa

Abstract

Herein, we describe the batch and fixed-bed column adsorption of Cu^{2+} and Pb^{2+} by raw and treated date palm leaves (DP) and orange peel (OP) waste biomass. Contact time, pH, adsorbent dose, and particle size were optimized in batch adsorption experiments, while breakthrough curves obtained in fixed-bed adsorption experiments were used to determine the effects of bed height, initial metal concentration, particle size, and flow rate. The use of treated DP and/or OP in batch adsorption mode increased the removal efficiency of metal ions by 20–30% compared to that observed for raw adsorbents. The equilibration time was estimated as 0.5 h, with rapid metal removal observed during the first 15 min at an optimum pH value of ~5. Increasing the adsorbent dose from 0.5 to 6–7 g enhanced the metal removal efficiency by ~60%, whereas a particle size increase from 50 to 300 µm decreased this value by about 30% for both Cu^{2+} and Pb^{2+} and both raw and treated DP/OP. Both breakthrough and exhaust times increased with increasing bed height of the fixed-bed column, and the effect observed for treated DP exceeded that observed for raw DP by a factor of two. Conversely, both breakthrough and exhaust times decreased with increasing initial metal concentration, particle size, and flow rate. Increasing the particle size from 100–150 to 300 µm changed the exhaust time by 8 h when treated DP was used for Pb^{2+} adsorption. The obtained linear regression coefficients (R^2 = 0.9–0.99) suggest that both Thomas and Yoon–Nelson models are well-suited for predicting the adsorption performance of the present system.

Keywords: adsorption, date palm, fixed bed, orange peel, pre-treatment, Thomas, Yoon-Nelson

1. Introduction

Mitigation of the rapidly progressing contamination of aquatic environments with heavy metals has recently become a challenge for researchers (Han *et al.*, 2006; Sternberg and Dorn, 2002), being attributed to the daily disposal of extremely large quantities of untreated wastewater from industrial, agricultural, and household sources into natural water bodies (oceans, rivers, and lakes). The above wastewater can contain acids, plating metals, and toxic chemical residues, with heavy metals being of particular concern due to their long-term persistency in soils and sediments. Since heavy metals are not biodegradable, they can accumulate in the environment and the food chain, posing severe health hazards to humans, animals, and plants (Singh *et al.*, 2011). Excessive exposure to heavy metals can result in cancer, retarded growth and development, organ damage, elevated blood pressure and blood sugar levels, joint diseases, and, in extreme cases, sudden death (Chary *et al.*, 2008; Titi and Bello, 2015).

Among toxic metals, the major environmental contaminants present in drinking water and industrial wastewater are copper and lead (Osman *et al.*, 2010; Soliman *et al.*, 2016), originating from battery manufacturing waste, erosion of natural deposits, leather finishing, and metal plating (Song *et al.*, 2013). The maximum allowable limits for copper and lead in discharged wastewater set by the Environmental Protection Agency (EPA) equal 1.3 and 0.05 mg L^{-1}, respectively (Barakat, 2011; Djeribi and Hamdaoui, 2008; Zahra, 2012). Hence, methods of controlling and reducing the levels of these metal ions in wastewater to comply with EPA guidelines are urgently required to maintain a sustainable global ecosystem (Ertaş and Öztürk, 2013).

The removal of heavy metals from (waste)water has been attempted using various physical, chemical, and biological techniques, e.g., reverse osmosis (Gupta *et al.*, 2012), hybrid electrocoagulation membranes (Mavrov *et al.*, 2006), chemical precipitation, ion exchange (Dąbrowski *et al.*, 2004), chemical coagulation and flocculation (Amuda *et al.*, 2006), ozonation, hybrid flotation/membrane filtration (Blöcher *et al.*, 2003), and advanced oxidation (Oller *et al.*, 2011). However, these techniques are not widely used due to their high energy cost, production of oxidation by-products, and membrane fouling during filtration. Most of these methods

are also ineffective for metal ion concentrations of 10–100 mg L^{-1} (Bulut and Tez, 2007). Hence, extensive research efforts are now focused on developing new, cost-effective, and eco-friendly techniques for removing such toxic pollutants.

Biosorption is a technology developed in the last few years to mitigate contamination by toxic metals, presenting a potential alternative to traditional water decontamination treatment due to its low cost, abundant raw materials, minimal utilization of chemicals, generation of minimal amounts of biological sludge waste, and absence of nutrient requirements (Aksu, 2005; Sarı *et al.*, 2007). The efficiency of biosorption relies on the adsorption of dissolved metal ions onto the adsorbent surface. Recently, agricultural waste and byproducts such as tobacco stems, peat, wood, pine cones, banana peels, cotton balls, coffee leaves, wheat straws, rice husk, sawdust, and orange peel have been widely investigated as sorbents for metal removal from (waste)water (Annadurai *et al.*, 2003; Ho *et al.*, 2002; Momcilovic *et al.*, 2011; Riaz *et al.*, 2009; Saka *et al.*, 2012; Sciban *et al.*, 2007; Tan, 1985; Wong *et al.*, 2003), making this process both cost-effective and environmentally friendly and simultaneously helping to reduce surface pollution.

Saudi Arabia is the biggest market for oranges and dates, which are important fruit crops occupying a large percentage of cultivated land. Three large Saudi Arabian cities (Riyadh, Jeddah, and Dammam) annually produce more than six million tons of biowaste, with values of 600,000 kg/day observed during pilgrimage and local fasting festivals (Khan and Kaneesamkandi, 2013). A large fraction of the generated food left-overs is represented by orange and date palm waste. On average, about 20 million kg of date palm waste (leaves and stems) is produced annually as a result of farming practices (such as thinning and pruning) and disease treatment. Similarly, a large amount of orange peel waste is produced by domestic orange juice industries. These biomass wastes can potentially be used as low-cost green adsorbents for removing lead and copper from wastewater, helping reduce surface pollution and decontaminate aqueous media.

In this study, we focused on the removal of copper (Cu^{2+}) and lead (Pb^{2+}) using both raw and treated (i.e., chemically modified) date palm leaves (DP) and orange peel (OP) waste biomass employing batch and fixed-bed methods. The removal efficiencies of Cu^{2+} and Pb^{2+} achieved by the above low-cost agricultural byproducts were determined in batch experiments, whereas the industrial-scale applicability of these sorbents was analyzed in fixed-bed column experiments. All experiments were carried at room temperature by varying certain parameters while keeping other ones constant. Finally, the process of column adsorption was analyzed using different kinetic models for estimating the breakthrough performance of the fixed-bed column reactor.

2. Materials and methods

2.1. Chemicals and adsorbents

Stock solutions of Cu^{2+} and Pb^{2+} (1000 mg/L each) in deionized water were prepared by dissolving appropriate amounts of copper sulfate pentahydrate ($CuSO_4{\cdot}5H_2O$; AR grade, Merck, Germany) and lead nitrate ($Pb(NO_3)_2$, Tianjin Benchmark Chemical Reagent Co., Ltd. Tianjin, China) in a 1000-mL volumetric flask, respectively. The solution pH was adjusted using aqueous HCl or NaOH (0.1 M each), and pH measurements were carried out utilizing a microprocessor-based pH meter (PHS-3CW, China). Stock solutions were stored at 4 °C for long-term use, with 2 mL of concentrated HCl added as a preservative. Different standard solutions with initial concentrations of 50−150 mg/L were prepared from stock solutions by serial dilution with deionized water.

To prepare raw adsorbents, both DP and OP were collected from various locations in Riyadh, Saudi Arabia, and were initially washed with tap water and thoroughly rubbed to remove all foreign particles. The adsorbents were further washed with distilled water, filtered, and placed in a drying oven held at ~70 °C for 24 h. The dried materials were crushed by a crushing machine and ground (Planetary Mono Mill Pulverisette 6, FRITSCH, Germany) to an average particle size of 0.045–0.3 mm.

To obtain pre-treated adsorbents, ~50-g samples of raw DP and OP were reacted with 250 mL of 1% ethanolic NaOH at room temperature (25 °C) for 24 h. Further modification was performed by stirring approximately 30 g of the dry product in 1 L of 1% mercaptoacetic acid ($C_2H_2O_2S$) for 12 h at room temperature to improve adsorption capacity, as reported earlier (Amin *et al.*, 2016).

2.2. Batch adsorption experiments

Batch adsorption experiments were performed to measure the effectiveness of Cu^{2+} and Pb^{2+} adsorption for both raw and treated DP and OP. These experiments were carried out in duplicate, utilizing 100-mL conical flasks and an orbital shaking incubator (Wise Cube Orbital Shaker, Daihan Scientific Co. Ltd., Wisd. ThermoStable IS-20, South Korea) at a certain controlled temperature and 220 rpm. Samples were drawn every 5 min, centrifuged (Elektromag M815P) at 1000 rpm, and filtered through a nitrocellulose filter (0.45 µm) using a vacuum filtration assembly. The filtrates were diluted to obtain metal levels corresponding to the linear range of calibration curves and were analyzed using a flame atomic absorption spectrometer (Perkin Elmer AAnalyst 200). Batch adsorption data were analyzed using Eqs. (1) and (2) to obtain the adsorption capacity and the removal effectiveness of selected heavy metal ions.

$$q_e = \left(\frac{C_0 - C_f}{m}\right) V \quad (1)$$

$$\text{Removal efficiency } (\%) = \left(\frac{C_0 - C_f}{C_0}\right) \times 100 \quad (2)$$

where q_e is the metal uptake (mg g^{-1}), C_0 is the initial metal concentration (mg L^{-1}), C_f is the residual metal concentration (mg L^{-1}) after adsorption, and V (L) and m (g) are the volume of the heavy metal–containing solution and adsorbent mass, respectively.

Fixed raw and treated adsorbent masses of 0.5 and 1 g $^{-}$per litre of the heavy metal ion's solution, respectively, were used in different experiments. To determine the equilibration time, batch experiments were conducted at regular time intervals during the first 3 h. Similarly, batch adsorption experiments were also performed to optimize the contact time, pH, adsorbent dose, adsorbent particle size, and the pre-treatment procedure. Table 1 summarizes the results of batch experiments and the used parameters.

2.3. Column adsorption

Fixed-bed column adsorption experiments were carried out in a cylindrical glass column with an internal diameter of 2.5 cm and a height of 60 cm. The top and bottom of the column were covered with a 3-mm layer of glass beads and glass wool, respectively, and the column was filled with adsorbents to a bed height of ~50 cm. Adsorbents with different particle sizes were used, as specified for each experiment in Table 2. In every experiment, a heavy metal–containing solution of a certain initial concentration (50–150 mg L^{-1}) was pumped to the top of the column using a peristaltic pump at a fixed flow rate (2–10 L min^{-1}), as shown in Table 2. All experiments were carried out at room temperature and had a pH of 4–5 (Table 2). Samples for determining the concentration of metal ions were collected at regular time intervals at the bottom of the column, and continuous adsorption experiments were stopped only after the column was fully exhausted. After plotting the breakthrough curves (C_t/C_0 vs. time), the 50% breakthrough capacity (i.e., C_t/C_0 = 0.5) was calculated using Eq. (3):

$$Q_{0.5} = \frac{(t_{0.5} \times Q \times C_0)}{m} \quad (3)$$

where $Q_{0.5}$ is the 50% breakthrough capacity (mg of metal adsorbed per gram of adsorbent, mg g^{-1}), $t_{0.5}$ is the breakthrough time at 50% (i.e., at C_t/C_0 = 0.5), C_0 and C_t are the initial and effluent metal concentrations (mg L^{-1}), respectively, and Q (mL min^{-1}) and m (g) are the flow rate and adsorbent mass, respectively. Finally, the obtained data were analyzed using Thomas and Yoon-Nelson kinetic models as well as the bed depth service time (BDST) model to determine the kinetic parameters, adsorption capacity, and breakthrough performance of the utilized fixed-bed column reactor.

3. Results and discussion

3.1. Surface characterization of adsorbents

The availability of pores and internal surfaces was determined by scanning electron microscopy (SEM, Tescan Vega 3 SBU, USA), with images of raw/treated adsorbents before and after Cu^{2+}/Pb^{2+} adsorption at different magnifications (×2400, ×3000, and ×6000) shown in Fig. 1. Images in Figs. 1a and 1b show raw DP and OP surfaces before adsorption.

After adsorption, the pores were covered by heavy metal ions (Figs. 1c and 1d), making their structural analysis complicated. Prior to adsorption, however, rough asymmetric pores with different diameters and cylinders were observed on the surface of both adsorbents, which improved their interactions with heavy metal ions. Cylindrical shaped structures seem to be composed of multicellular fibres bound together by lignin. One can also observe the central void inside the fibre, known as the lumen (Fig. 1a). Secondary pores were also seen inside the primary pores on the surface of both adsorbents before the adsorption of heavy metal ions. These primary and secondary pores were critical for the sorption of heavy metal ions.

The surfaces of both raw and treated DP exposed to heavy metal solutions exhibited closed pore structures and a smooth and shiny appearance owing to the physicochemical interaction between the above ions and the functional groups present on the rough surface of these adsorbents. The attachment of metal ions could be seen clearly on the surface of the adsorbents and inside the pores and the change of the structure of adsorbents after adsorption can be linked to the influence of metal ions.

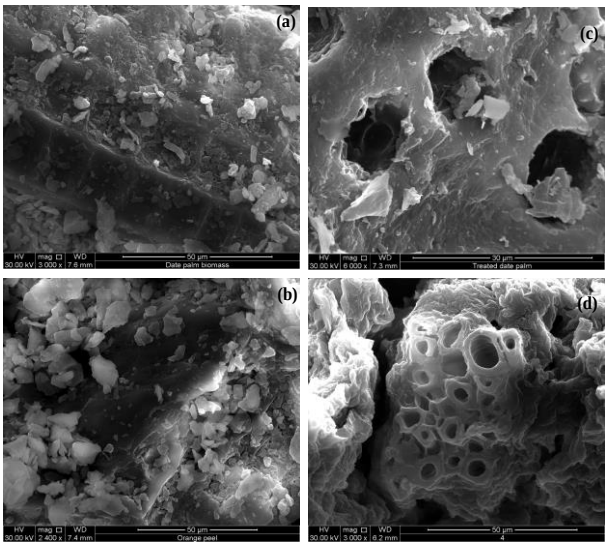

Figure 1. SEM images of (a) raw DP, (b) raw OP, (c) treated DP after Cu^{2+} adsorption, and (d) treated OP after Pb^{2+} adsorptionResults and discussion

3.2. Analysis of batch adsorption data

Batch experiments were performed to measure the adsorption effectiveness of specific metals. In this section, the selected results for the potential of raw and treated DP/OP for removing Cu^{2+} and Pb^{2+} in batch systems is presented. The effects of different process variables

including pre-treatment effects, contact time, pH, adsorbent dose, and particle size were investigated while keeping other relevant process parameters constant, as shown in Table 1.

Table 1. Selected process variables and constants used in different batch experiments

Variable parameters	Value/range	Adsorbent/metal	Constant parameters				
			Contact time, min	pH	Initial metal conc. mg L^{-1}	Adsorbent dose, g	Particle size, µm
Pre-treatment		Raw and treated DP/Cu^{2+}	-	5	50	1	45
		Raw and treated OP/Pb^{2+}					
Contact time, min	0–1500	Treated DP and OP/Cu^{2+}					
		Raw DP and OP/Pb^{2+}					
Initial solution pH	2–6	Raw DP/Cu^{2+}	15	-	50	1	75
		Treated OP/Pb^{2+}					
Adsorbent dose, g	0.5–7	Raw DP/Cu^{2+}	15	5	50	-	75
		Treated OP/Pb^{2+}					
Particle size, µm	50–300	Raw and treated DP/Cu^{2+}	15	5	50	1	-
		Raw and treated OP/Pb^{2+}					

3.2.1. Effects of pre-treatment and contact time on metal adsorption efficiency

The effects of pre-treatment (i.e., chemical modification) on the Cu^{2+} and Pb^{2+} adsorption capacities of raw DP and OP, respectively, are shown in Fig. 2. Batch adsorption experiments for determining pre-treatment effects were performed at an initial metal concentration of 50 mg L^{-1}, adsorbent dose of 1 g, adsorbent particle size of 45 µm, and an initial solution pH of 5 (Table 1).

After ~3 h of adsorption, a 20 % higher Cu^{2+} removal efficiency was observed for treated DP compared to that of raw DP, with this difference slightly increasing after 1 d. Similarly, treated OP exhibited a ~30% higher Pb^{2+} adsorption efficiency than raw OP (Fig. 2b). The observed adsorption enhancement was attributed to the increased number of functional groups generated on the surface of modified adsorbents (Abia *et al.*, 2002). Moreover, the pre-treatment or chemical modification of raw/natural biosorbents was reported to improve the adsorption capacity by enhancing adsorbent porosity and stability as well as by controlling the coloration and release of organic materials in solution (Ali *et al.*, 2014; Jiménez-Cedillo *et al.*, 2013; Mohan and Pittman, 2007; Zhu *et al.*, 2008; Khosa *et al.*, 2013).

To establish an equilibrium, which is essential for designing batch adsorption experiments, it was important to evaluate the effect of contact time on Cu^{2+} and Pb^{2+} adsorption capacity. Kinetic measurements were conducted to determine the time required to reach adsorption equilibrium, with results obtained for the removal of Cu^{2+} with treated DP/OP and that of Pb^{2+} using raw DP/OP presented in Fig. 3. As described in Table 1, a pH of 5, an initial metal concentration of 50 mg L^{-1}, an adsorbent dose of 1 g, and particle size of 45 µm was used.

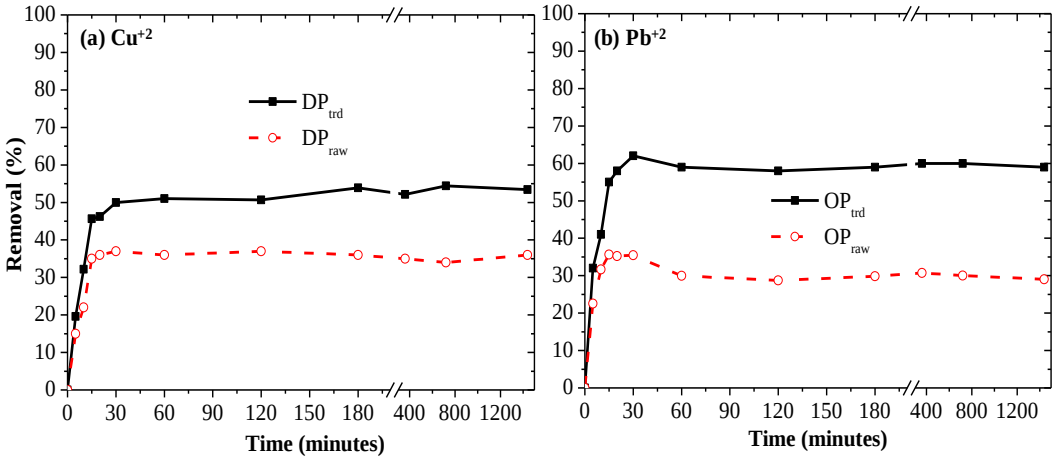

Figure 2. Effects of pre-treatment on the removal of (a) Cu^{2+} by DP and (b) Pb^{2+} by OP

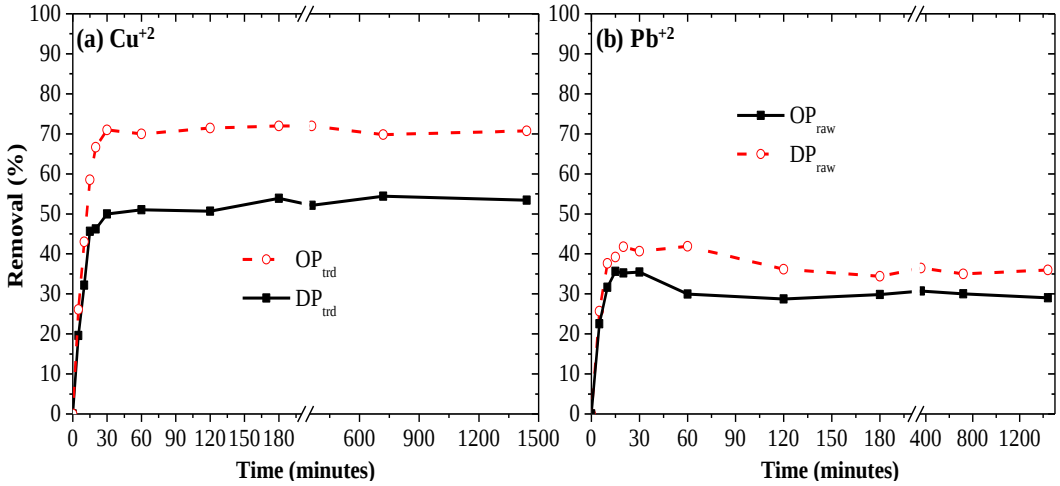

Figure 3. Effects of contact time on the removal of (a) Cu^{2+} and (b) Pb^{2+} by DP and OP

Figure 3 shows the effect of contact time on the adsorption of Cu^{2+} and Pb^{2+} by raw and treated DP and OP, revealing rapid adsorption during the first 15–20 min that was ascribed to the availability of unreacted adsorbent surface at the initial stage (Qadeer and Akhtar, 2005). Cu^{2+} and Pb^{2+} adsorption equilibria were established in ~30 min, although the efficiency of Pb^{2+} removal by raw DP/OP was less (35–40%) than that of Cu^{2+} removal by treated DP/OP (50–70%). For other batch experiments, an equilibration time of 30 min was used to optimize the adsorption process.

3.2.2. Effects of pH and adsorbent dose

pH variation significantly influences the adsorption mechanism, resulting in efficient removal of cationic molecules by biosorbents (Areco and Afonso, 2010). The effect of initial solution pH was investigated in the range of 2 to 6 (Fig. 4a), while other parameters, i.e., initial metal concentration (50 mg L^{-1}), adsorbent dose (1 g), particle size (75 µm), and contact time (15 min) were kept constant (Table 1). Figure 4b shows the effects of different adsorbent doses (0.5 to 7 g), with other parameters being constant, at an initial solution pH of 5.

The maximum efficiency of Cu^{2+} removal by raw DP was observed at pH of 5, whereas the corresponding efficiency of Pb^{2+} removal by treated OP was maximal at pH of 5–5.5 (Fig. 4a). The maximum adsorption capacity was estimated as 17.5 and 28 mg g^{-1} for Cu^{2+} and Pb^{2+} using raw DP and treated OP, respectively. Similar pH dependencies have previously been investigated for the adsorption of heavy metal ions onto plant wastes of various types (Yadav *et al.*, 2015; El Nemr *et al.*, 2008; Rajamohan *et al.*, 2014). The enhanced removal of Cu^{2+} and Pb^{2+} under acidic conditions was ascribed to the competition between metal cations and protons (H^+) for biosorption sites and increased electrostatic repulsive interactions at low pH (Chieng *et al.*, 2015; El-Bindary *et al.*, 2014).

The adsorbent dose influences the economic viability of the adsorption process, making it critical to achieve maximal removal efficiency using a minimal amount of adsorbent.

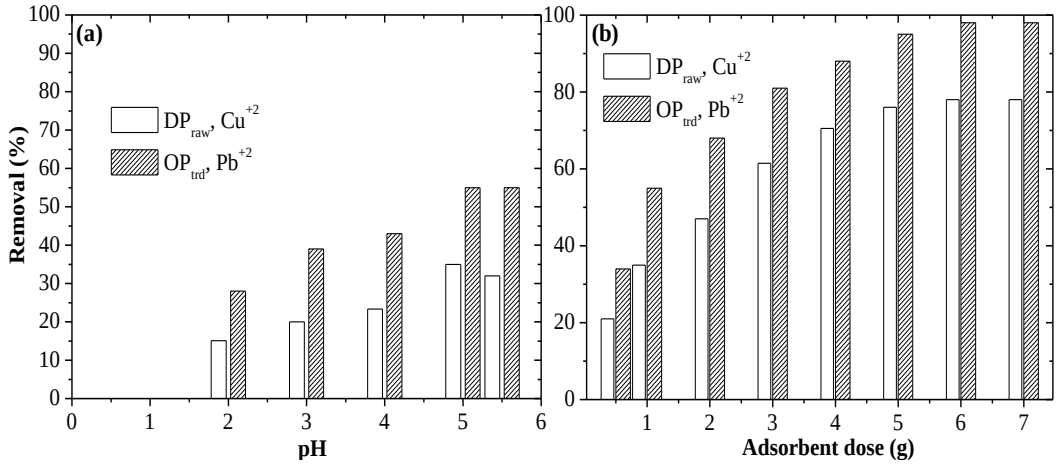

Figure 4. Effects of (a) pH and (b) adsorbent dose on the removal of Cu^{2+} and Pb^{2+} by DP and OP

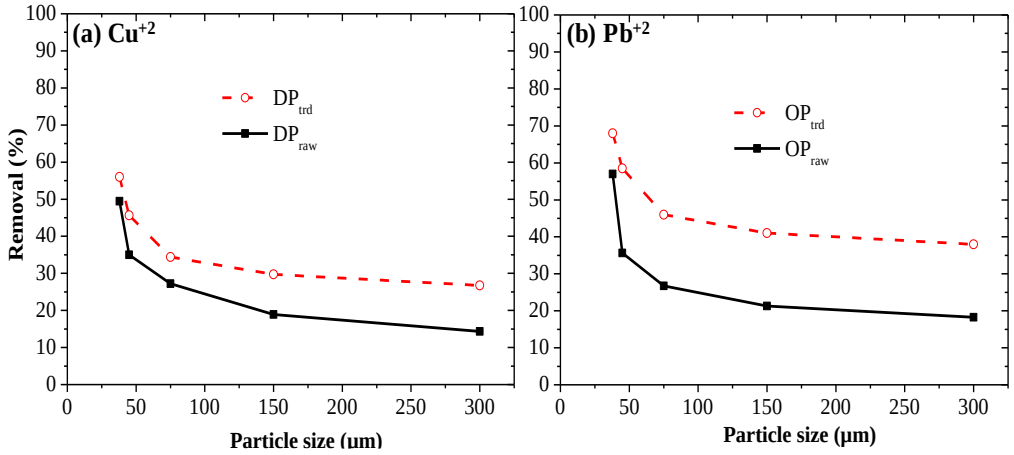

Figure 5. Effects of particle size on the removal of (a) Cu^{2+} by DP and (b) Pb^{2+} by OP

A 60–70% increase of metal removal efficiency was observed for Cu^{2+} by raw DP and for that of Pb^{2+} by treated OP when the adsorbent dose was increased from 0.5 to 5–7 g (Fig. 4b).

The enhanced removal efficiency of both Cu^{2+} and Pb^{2+} at an adsorbent dose of 5–7 g, as compared to those observed at lower dosages of 1–4 g, was attributed to the larger available surface area with more binding sites in the former case (Aydın *et al.*, 2008; Uzunoğlu *et al.*, 2014). The stable removal efficiencies beyond 5 g shows that this value is the optimum dose of both adsorbents and was estimated as 5 g at which the maximum adsorption capacity of 38 and 49 mg g^{-1} was recorded for Cu^{2+} and Pb^{2+} using raw DP and treated OP, respectively.

The maximum adsorption of both metal ions was observed at contact times of about 10 min when the dose increased to 6-7 g using same values of other process parameters. Increasing the adsorbent dose increased the adsorption capacity, concomitantly increasing the removal efficiency, as reported in previous studies (Yadav *et al.*, 2013; Hilal *et al.*, 2012; Boudrahem *et al.*, 2011; Ghorbani *et al.*, 2012; Hikmat *et al.*, 2014; Haleem and Abdulgafoor, 2010).

3.2.3. Effects of particle size

The effects of particle size were investigated for the removal of Cu^{2+} by raw and treated DP and for that of Pb^{2+} by raw and treated OP, as shown in Figs. 5a and 5b, respectively, with initial metal concentration (50 mg L^{-1}), adsorbent dose (1 g), pH (5), and contact time (15 min) kept constant, and the average particle size varied between 50 and 300 µm (Table 1).

As shown in Fig. 5, increasing the particle size from 50 to 300 µm decreased the removal efficiency of both Cu^{2+} and Pb^{2+} by ~30–35%, which could be ascribed to the decreased adsorbent surface area and number of available binding sites (Al-Ghouti *et al.*, 2010). Moreover, larger particles are known to result in increased internal diffusion related to adsorbate penetration, delaying the establishment of an equilibrium and consequently decreasing adsorption capability.

Table 2. Selected process variables and constants used in different fixed-bed column experiments

Variable parameters	Value/range	Adsorbent/metal	Constants parameters					
			Contact time, h	pH	Bed height, cm	Initial metal conc., mg L^{-1}	Particle size, µm	Flow rate, mL min^{-1}
Bed height, cm	5, 10, 15	Raw DP/Cu^{2+}	6.67	4	-	100	300	2
	5, 10	Raw DP/Pb^{2+}	10.83	5				
		Treated DP/Pb^{2+}	21.67			50		4
Initial metal conc., mg L^{-1}	50, 100, 150	Raw DP/Cu^{2+}	6.67	4	5	-	300	2
	100, 200	Raw DP/Pb^{2+}	10.83	5			150	
	50, 100	Treated DP/Pb^{2+}	21.67				300	
Particle size, µm	150, 300	Raw DP/Pb^{2+}	10.83	5	5	100	-	4
	100, 200, 300	Treated DP/Pb^{2+}	21.67					
Flow rate, mL min^{-1}	4, 7, 10	Raw DP/Cu^{2+}	6.67	5	5	100	300	-
	2, 4, 6	Treated DP/Pb^{2+}	21.67			50		

3.3. Fixed-bed column adsorption

The continuous adsorption of Cu^{2+} and Pb^{2+} in a fixed-bed column was investigated using both raw and treated DP and OP, however only selective results are presented in this section. Breakthrough curves (plots of normalized concentration (C_t/C_0) vs. time) under specified operating conditions were predicted for the successful design and operation of fixed-bed adsorption. The shape of these curves and breakthrough times are important characteristics influenced by individual transport in the column and the adsorbent, reflecting the loading behavior of the heavy metal ions being removed (Vázquez *et al.*, 2006; Guo and Lua, 2003; Ahmad and Hameed, 2010). The effects of parameters such as bed height, initial metal concentration, particle size, and flow rate were evaluated separately by keeping the values of other relevant parameters constant, as shown in Table 2

3.3.1. Effects of bed height

The effects of bed height (5, 10, and 15 cm) on the adsorption of Cu^{2+} by raw DP and on that of Pb^{2+} by raw and treated DP were investigated for solutions with initial pH values of 4–5 and initial metal concentrations of 50 and 100 mg L^{-1} at flow rates of 2 and 4 mL min^{-1} and an adsorbent particle size of 300 µm (Fig. 6). Figure 6a shows that increasing the bed height from 5 to 15 cm resulted in a slight breakthrough time increase of ~0.5 h for Cu^{2+} adsorption by raw DP, whereas the exhaust time was increased by ~3 h. A similar insignificant breakthrough time increase and nearly unchanged exhaust time were observed for the adsorption of Pb^{2+} by raw DP when the bed height was doubled from 5 to 10 cm, as shown in Fig. 6b. However, when treated DP was used for the adsorption of Pb^{2+}, a breakthrough time increase of ~1 h and a significant exhaust time increase of more than 6 h were observed (Fig. 6c). The increased breakthrough and exhaust times observed for deeper beds are attributed to their increased surface area and a larger amount of binding sites for heavy metal ions. Similar results were reported for adsorption of Cu^{2+} by magnetized sawdust (Kapur and Mondal, 2016), in line with other investigations on the adsorption of different dyes onto plant-based adsorbents (Yagub *et al.*, 2015; Sajab *et al.*, 2015).

3.3.2. Effect of initial metal concentration

Breakthrough curves obtained for different initial metal concentrations (50–200 mg L^{-1}) at a constant flow rate (2 mL min^{-1}) and a bed height of 5 cm are shown in Fig. 7. Adsorption of Cu^{2+} onto raw DP was conducted at an initial solution pH of 4 and an adsorbent particle size of 300 µm (Fig. 7a), whereas adsorption of Pb^{2+} by raw and treated DP was performed at an initial pH value of 5 and adsorbent particle sizes of 150 and 300 µm, respectively. For the adsorption of Cu^{2+} onto raw DP, increasing the initial metal concentration from 50 to 150 mg L^{-1} decreased the breakthrough and exhaust times by ~30 and 90 min, respectively (Fig. 7a). A similar decrease of breakthrough time (about 30 min) and exhaust time (more than 2 h) was observed for the adsorption of Pb^{2+} onto raw DP when the initial metal concentration was increased from 100 to 200 mg L^{-1} (Fig. 7b). When treated DP was used, the decreases of breakthrough and exhaust times was observed as ~ 1 h and > 6 h, respectively, as the initial Pb^{2+} concentration was increased from 50 to 100 mg L^{-1} (Fig. 7c).

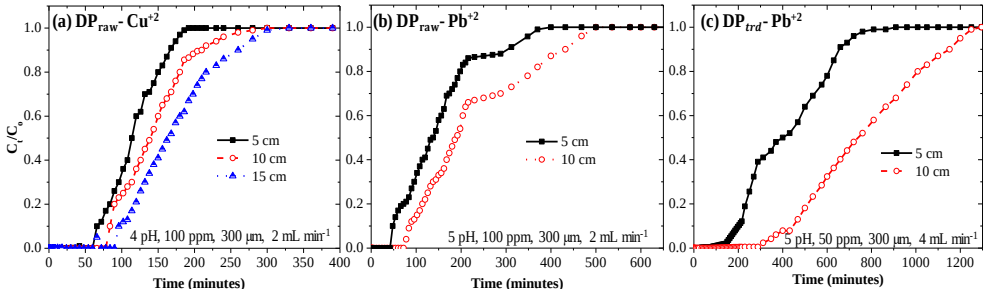

Figure 6. Effects of bed height on the adsorption of (a) Cu^{2+} by raw DP and Pb^{2+} by (b) raw and (c) treated DP.

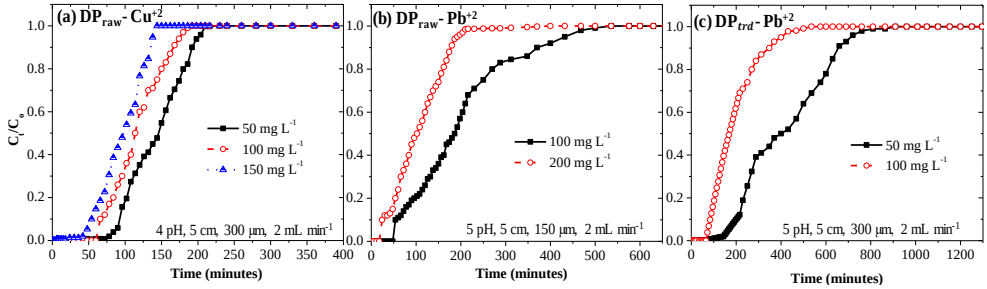

Figure 7. Effects of initial metal concentration on the adsorption of (a) Cu^{2+} by raw DP and Pb^{2+} by (b) raw and (c) treated DP

The above breakthrough time decline observed for increasing initial metal concentrations was attributed to slower mass transport caused by the reduced metal concentration gradient, which consequently decreased the diffusion or mass transfer coefficient (Teng and Lin, 2006).

3.3.3. Effects of particle size

The effects of average particle size on the adsorption of Pb^{2+} onto raw and treated DP are exemplified by the breakthrough curves in Figs. 8a and 8b, respectively, which were recorded at constant pH (5), bed height (5 cm), initial metal concentration (100 mg L^{-1}), and flow rate (4 mL min^{-1}), as shown in Table 2.

No influence of particle size on breakthrough time was observed when raw DP was used for Pb^{2+} adsorption. However, the exhaust time was decreased by 2 h when larger particles (300 µm) were used, as compared to the case when smaller particles (150 µm) were employed (Fig. 8a). For adsorption of Pb^{2+} onto treated DP, both breakthrough and exhaust times decreased by almost 0.5 and 8 h, respectively, as the average particle size increased from 100 to 300 µm (Fig. 8b). The left-to-right breakthrough curve shift with decreasing particle size resulted in enhanced metal ion removal. Consequently, the increased breakthrough and exhaust times observed for smaller particle sizes imply that the column is more difficult to exhaust under these conditions than in the case of larger particles.

3.3.4. Effects of flow rate

The adsorption of Cu^{2+} and Pb^{2+} at flow rates in the range of 2–10 mL min^{-1} was studied using raw and treated DP, respectively, with breakthrough curves shown in Fig. 9 An initial solution pH of 5 with a bed height of 5 cm and an average particle size of 300 µm was used, whereas initial metal concentrations of 100 and 50 mg L^{-1} were used for Cu^{2+} and Pb^{2+}, respectively.

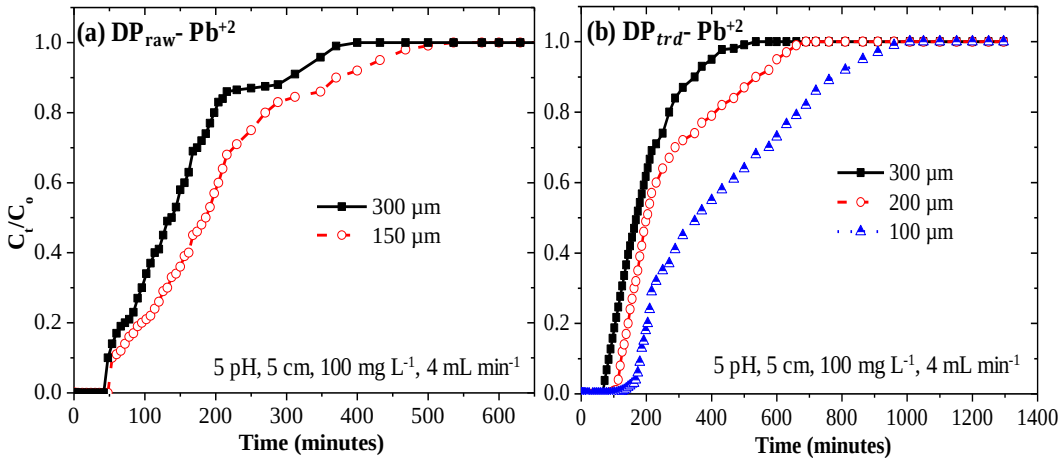

Figure 8. Effects of particle size on the adsorption of Pb^{2+} by (a) raw and (b) treated DP

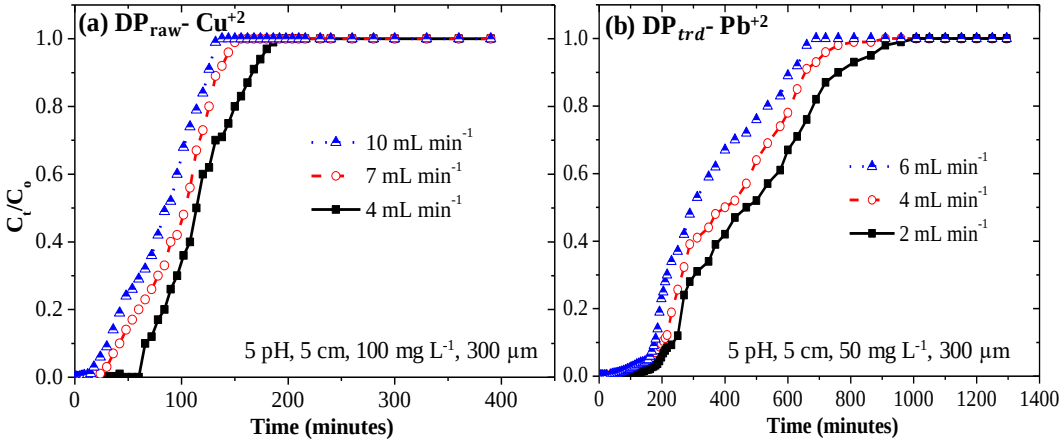

Figure 9. Effects of flow rate on the adsorption of (a) Cu^{2+} by raw DP, and (b) Pb^{2+} by treated DP.

The breakthrough and exhaust times for Cu^{2+} adsorption onto raw DP were decreased by slightly less than 1 h by increasing the flow rate from 4 to 10 mL min^{-1} (Fig. 9a). Similarly, both breakthrough and exhaust times gradually decreased by

slightly more than 1 h and ~4 h, respectively, for Pb^{2+} adsorption onto treated DP as the flow rate was increased from 2 to 6 mL min^{-1} (Fig. 9b). This result shows that the column is difficult to exhaust at smaller flow rates due to the higher removal efficiency of heavy metal ions in the bed. Besides, the low contact time between adsorbents and heavy metal ions observed at higher flow rates can reduce the adsorption efficiency of the packed bed. Furthermore, the faster adsorption zone movement at high flow rates may reduce the time for Cu^{2+}/Pb^{2+} adsorption onto the surface of packed DP/OP in the fixed-bed column (Sadaf *et al.*, 2015).

3.4. Breakthrough curve prediction and column adsorption models

3.4.1. Thomas model

The Thomas model, based on the Langmuir adsorption/desorption model and second-order reversible reaction kinetics, is most commonly used to describe the behavior of breakthrough curves in fixed-bed columns (Thomas, 1944; Futalan *et al.*, 2011; Apiratikul and Pavasant, 2008), being helpful for predicting the maximum adsorption capacity of adsorbents required for treatment plant design. This model was applied to calculate the maximum solid-phase concentrations of Cu^{2+}/Pb^{2+} and the corresponding adsorption rate constants using the data obtained for the fixed-bed column in continuous mode. The linearized form of the Thomas model can be expressed as Eq. (4):

$$\ln\left(\frac{C_0}{C_t}-1\right)=\frac{K_{Th}q_0m}{Q}-(K_{Th}C_0)t \quad (4)$$

where the Thomas rate constant or kinetic coefficient (K_{Th}, L min^{-1} mg^{-1}) and the maximum or equilibrium sorption capacity of the fixed-bed column (q_0, mg g^{-1}) can be determined from the plot of $\ln[(C_0/C_t)^{-1}]$ vs. time (t, min) at a given flow rate using linear regression analysis. In the above formula, C_0 and C_t are the initial and effluent metal concentrations (mg L^{-1}), Q is the flow rate (mL min^{-1}), and m is the amount of adsorbent in the column (g). Both K_{Th} and q_0 calculated from linearized plots were used to describe the column behavior (Pilli *et al.*, 2012). For adsorption of Cu^{2+} in a fixed-bed column packed with raw DP, K_{Th} increased and q_0 decreased with increasing flow rate (Table 3a). Table 3b presents the results of Pb^{2+} adsorption onto treated DP, showing that q_0 increased and K_{Th} decreased with increasing initial metal concentration, which can be attributed to the increased driving force related to the concentration difference between the metal ions onto the surface of the adsorbent and in the solution (Aksu and Gönen, 2004; Malkoc *et al.*, 2006). Moreover, K_{Th} and q_0 decreased with increasing bed height although the difference in q_0 was not significant by increasing the bed height from 5 to 15 cm (Table 3a). The diminution in the equilibrium sorption capacity with decrease in bed height signifies that the effluent concentration ratio of heavy metal ions increased more rapidly at smaller bed height than for a higher bed height. Hence, the lower bed depth improve the adsorption of both heavy metal ions on the studies adsorbents to a limited extent and the bed is saturated in less time for smaller bed heights which corresponds to less amount of adsorbent. These results are similar to those obtained by other researchers (Futalan *et al.*, 2011; Cheraghi *et al.*, 2016; Kapur and Mondal, 2016).

Table 3a. Thomas model parameters obtained by regression analysis at various conditions of Cu^{2+} adsorption onto raw DP.

Initial conc. (mg L^{-1})	**Bed height (cm)**	**Flow rate (mL min^{-1})**	**K_{Th} (mL min^{-1} mg^{-1})**	**q_0 (mg g^{-1})**	**R^2**
50	5	3	0.508	1.657578	0.9077
100	5	3	0.173	4.416846	0.9817
100	10	3	0.09	3.659286	0.9531
100	15	3	0.068	3.415889	0.8765
100	5	7	0.385	3.077403	0.9033
100	5	10	0.42	2.253571	0.891
150	5	3	0.165	5.190193	0.8847

Table 3b. Thomas model parameters obtained by regression analysis at various conditions of Pb^{2+} adsorption onto treated DP.

Initial conc. (mg L^{-1})	Bed height (cm)	Flow rate (mL min^{-1})	K_{Th} (mL min^{-1} mg^{-1})	q_0 (mg g^{-1})	R^2
50	5	2	0.148	7.647201	0.8539
100	5	2	0.049	9.63586	0.891
100	10	2	0.033	6.962264	0.8871
50	5	4	0.16	5.366374	0.9396
50	5	6	0.194	3.477099	0.9466

These conditions can be attributed to the high driving force due to the high amount of heavy metal ions perforated into the packed bed of DP. Similar results have been reported earlier for the adsorption of phosphate and nitrate on waste solids (Olgun *et al.*, 2013). Thus, the adsorption of Cu^{2+} and Pb^{2+} onto raw and treated DP, respectively, can be enhanced

at higher initial concentrations, lower flow rates, and smaller bed depths. R^2 values of ~0.9 and high indicated an average to good fits of the adsorption data to the Thomas model suggesting that internal and external diffusion were not rate-limiting steps (Rao *et al.*, 2011; Aksu and Gönen, 2004; Cheraghi *et al.*, 2016).

3.4.2. Yoon-Nelson model

The Yoon-Nelson model, a simple theoretical model based on the theory of adsorption and probability of adsorbate breakthrough, was also used to investigate the breakthrough behavior of both Cu^{2+} and Pb^{2+} for raw and treated DP. This model is applicable to single-component adsorption systems and assumes that the rate of adsorption probability decrease for each adsorbate molecule is proportional to the probability of adsorbate adsorption and breakthrough on the adsorbent (YOON and NELSON, 1984). The linearized form of the Yoon-Nelson model can be expressed as:

$$\ln \frac{C_t}{C_o - C_t} = K_{YN}t - TK_{YN} \quad (5)$$

where K_{YN} is the Yoon-Nelson rate constant (min^{-1}), T is the time required for 50% adsorbate breakthrough (min), C_0 and C_t are the initial and effluent metal concentrations, respectively (mg L^{-1}), and t is the breakthrough (sampling) time (min). K_{YN} (slope) and T (= intercept/K_{YN}) can be determined from the plot of $\ln(C_t/(C_0 - C_t))$ vs. sampling time (t, min).

This model was applied to experimental data obtained at different flow rates (2–10 mL min^{-1}), initial metal concentrations (50, 70, and 100 mg L^{-1}), and bed depths (between 5 and 15 cm), with Tables 4a and 4b showing the results obtained for adsorption of Cu^{2+} onto raw DP and that of Pb^{2+} onto treated DP, respectively.

The above calculations show that K_{YN} increased with increasing initial metal concentration and flow rate, but decreased with increasing bed height. The values presented in Tables 4a and 4b indicate that the time required to achieve a 50% adsorbate breakthrough decreased with increasing initial metal concentration and flow rate, increasing with increasing bed height for adsorption of both Cu^{2+} and Pb^{2+} onto raw and treated DP.

Table 4a. Yoon-Nelson model's constants calculated for Cu^{2+} adsorption onto raw DP.

Parameter	K_{YN} (min^{-1})	T (min)	R^2	Percentage error
Initial conc. (mg L^{-1})				
50	0.0572	140.9423	0.9338	1.120879
100	0.0681	114.3805	0.9667	0.33373
150	0.0705	96.92057	0.9765	2.02165
Flow rate (mL min^{-1})				
3	0.0481	114.3805	0.9667	0.33373
7	0.0615	94.17236	0.938	1.570526
10	0.0637	82.18367	0.9142	2.741215
Bed height (cm)				
5	0.0481	114.3805	0.9667	0.33373
10	0.0321	138.5327	0.9944	1.048064
15	0.0287	166.9477	0.9799	1.05416

Table 4b. Yoon-Nelson model's constants calculated for Pb^{2+} adsorption onto treated DP.

Parameter	K_{YN} (min^{-1})	T (min)	R^2	Percentage error
Initial conc. (mg L^{-1})				
50	0.0125	440.192	0.9415	2.37023
100	0.0156	188.7756	0.9546	1.49175
Flow rate (mL min^{-1})				
2	0.0125	440.192	0.9415	2.37023
4	0.0138	314.8333	0.9238	1.96667
6	0.0144	267.7986	0.9985	1.7615
Bed height (cm)				
5	0.0156	188.7756	0.9546	0.49175
10	0.0097	441.7113	0.9588	1.4278

The enhanced rate of metal uptake at higher initial metal concentrations could be due to the competition between adsorbate molecules for adsorption sites, with similar results previously reported by other researchers (Han *et al.*, 2009; Hamdaoui, 2006; Bhaumik *et al.*, 2013). The rate constant extents were improved with increase in the flow rate whereas the T (min) showed the reverse trend. An opposite

behavior was seen for both of the rate constant extents and *T* (min) by increasing the bed depth from 5 to 15 cm. The longer time required for attaining the breakthrough or saturation in the greater bed depths of column is due to the large amount of adsorbent that provides a greater number of sites for the binding of heavy metal ions. On the other hand, columns with short bed height were saturated more quickly owing to lesser amount of adsorbent and the available binding sites. Similar pattern was reported in the previous research (Kapur and Mondal, 2016). The insignificant percentage error (describing the deviation of T values calculated using this model with experimental data ($\tau_{50\%\ exp.}$)) and high linear regression coefficients (R^2 = 0.9–0.99) indicate that the Yoon-Nelson model could well fit the experimental data.

3.4.3. BDST model

The BDST model, based on the Bohart-Adams equation modified by Hutchins, is the most simplified fixed-bed analysis method (El-Kamash, 2008; Hutchins, 1973; Santhy and Selvapathy, 2006; Lee *et al.*, 2001), predicting the relationship between bed height and service time while ignoring the resistances of external film and intraparticle mass transfer (Ko *et al.*, 2000). This model assumes that the rate of adsorption is controlled by the surface reaction between the adsorbate and the adsorbent with unused capacity (Goel *et al.*, 2005). Eq. (6) shows a linearized version of the BDST model (Sadaf and Bhatti, 2014; Baral *et al.*, 2009), describing the service time (*t*, min) at a breakthrough point:

$$t=\frac{N_b}{C_o U}z-\frac{1}{K_a C_o}\ln\left(\frac{C_o}{C_b-1}\right) \quad (6)$$

where *z* is the bed height (cm), C_0 and C_b are the initial and breakthrough concentrations of metals (mg L^{-1}), respectively, *U* is the linear velocity (cm min^{-1}), N_b is the bed biosorption capacity (mg L^{-1}), and K_a is the rate constant of the BDST model (L mg^{-1} min^{-1}). Thus, K_a and N_b can be determined from the slope (N_b/C_0U) and the intercept ($(1/K_aC_o)$ ln $[(C_0/C_t)^{-1}]$) of the linear plot of service time vs. bed height, respectively.

The breakthrough times for Pb^{2+} adsorption onto treated OP obtained for various bed heights (5, 7, 10, and 15 cm), initial metal concentrations (50, 100, and 150 mg L^{-1}), and flow rates (4, 7, and 10 mL min^{-1}) were introduced into the BDST model. The linear velocity *U* was calculated by dividing flow rate by the cross-sectional area of the fixed-bed column (diameter = 2.5 cm). BDST model parameters were also calculated for different initial metal concentrations at a fixed-bed height of 5 cm and a flow rate of 4 mL min^{-1} and for different flow rates at a fixed-bed height of 5 cm and an initial Pb^{2+} concentration of 100 mg L^{-1} (results not shown). Similarly, BDST model parameters calculated from the slopes and intercepts of linear plots for different bed heights at a fixed flow rate of 4 mL min^{-1} and an initial metal concentration of 100 mg L^{-1} are listed in Table 5.

Table 5. BDST model's parameters for adsorption of Pb^{2+} onto treated OP at various bed heights.

Bed height	N_b (mg L^{-1})	K_a	R^2
5	2313.309	0.203447	0.87
7	2545.455	0.18259	0.99
10	2769.455	0.149064	1
15	2973.091	0.135631	1

As the bed height increased from 5 to 15 cm, the volumetric sorption capacity of the bed (N_0) increased, and the rate constant (K_0) decreased, indicating that the breakthrough was delayed (Table 5). This behavior was probably due to the increased residence time of the metal solution inside the column, allowing the ions to diffuse deeper into the treated OP, as reported in earlier studies (Khitous *et al.*, 2016; Han *et al.*, 2007). The volumetric sorption capacity of the bed was also increased by increasing the flow rate and initial metal concentration, which, however, resulted in an increase and decrease of the BDST rate constant, respectively. The observed high correlation coefficients ($R^2 > 0.99$) indicate the validity of the BDST model for describing the adsorption of Pb^{2+} onto treated OP; however, a worse correlation was observed at a lower bed height (5 cm in Table 5).

4. Conclusions

This study revealed that locally available DP and OP can be used to remove Cu^{2+} and Pb^{2+} from aqueous solutions in both batch and continuous flow systems, i.e., fixed-bed columns. The effectiveness of pre-treatment was investigated by comparing the performances of raw and treated DP and OP. Batch adsorption experiments were carried out to optimize contact time, pH, adsorbent dose, particle size, and pre-treatment effects. Similarly, fixed-bed adsorption was analyzed using breakthrough curves under specified operating conditions to evaluate the effects of bed height, initial metal concentration, particle size, and flow rate.

For batch adsorption, a ~20% higher Cu^{2+} removal efficiency was observed for treated DP compared to that of raw DP. The use of treated OP also enhanced the adsorption of Pb^{2+} by ~30%, probably due to the increased number of functional groups present on the surface of modified adsorbents and their enhanced porosity and stability. The rapid adsorption observed during the first 15 min of contact could be linked to the availability of unused adsorbent surface area at the initial stage, and the equilibrium for Cu^{2+} and Pb^{2+} adsorption was established within 30 min. The removal of both Cu^{2+} and Pb^{2+} using raw and treated DP/OP was most efficient at pH 5–5.5.

The removal efficiencies of Cu^{2+} and Pb^{2+} were increased (by ~60–70%) by increasing the adsorbent dose from 0.5 to 6–7 g for both raw and treated adsorbents. A 30–35% decrease of the above removal efficiencies was observed when the particle size was increased from 50 to 300 µm.

For the adsorption of Cu^{2+} onto raw DP in a fixed-bed column, increasing the bed height from 5 to 15 cm resulted in a slight breakthrough time increase of about 30 min, as compared to the 3-h increase of exhaust time. However, both breakthrough and exhaust times for the adsorption of Pb^{2+} onto treated DP increased by 1 h and ~6 h, respectively, when the bed height was increased from 5 to 10 cm. An increase of initial metal concentration from 50 to 150 mg L^{-1} resulted in breakthrough and exhaust time decreases of ~30 and 90 min, respectively, for adsorption of Cu^{2+} onto raw DP. Doubling the initial concentration of Pb^{2+} from 50 to 100 mg L^{-1} resulted in breakthrough and exhaust time decreases of ~1 h and > 6 h, respectively, when treated DP was used. Both breakthrough and exhaust times decreased as the particle size was increased from 100–150 to 300 µm, with a significant decrease of ~8 h observed for exhaust time when treated DP was used for the adsorption of Pb^{2+}. Flow rate also affected the breakthrough and exhaust times, with an increase of about 4 mL min^{-1} resulting in decreases of ~1 and 4 h, respectively, when treated DP was used for the adsorption of Pb^{2+}.

The breakthrough performance and adsorption capacity for column adsorption were further evaluated using Thomas, Yoon-Nelson, and BDST models. R^2 values of 0.9 and higher were obtained for the Thomas model, showing an average-quality fit and suggesting that the rate-limiting steps were not related to internal and external diffusion. The insignificant deviation between *T* values calculated using the Yoon-Nelson model and experimental data, together with high R^2 values (0.9–0.99), indicated that this model fitted the experimental data well. Finally, close-to-unity R^2 values observed for the BDST model (except for lower bed heights) indicated the validity of this model for describing the adsorption of Pb^{2+} onto treated OP.

These results illustrated the successful application of both raw and treated DP and OP for adsorption of heavy metal ions and confirmed the possibility of using these agricultural wastes as adsorbents in continuous flow systems. The enhanced performance of treated DP and OP further supported the idea that suitable modifications/combinations can increase the number of functional groups on the adsorbent surface. In this context, future work should be directed at establishing suitable physical, chemical, and physicochemical surface modifications to further improve the adsorption capabilities of both adsorbents in column studies. These modifications can also make the naturally occurring functional groups available for adsorption, which may influence the removal of a particular metal from wastewater containing multiple heavy metals. However, from an economical point of view, the cost factor should be considered when selecting an adsorbent. This study leaves plenty of room for further investigation due to the complex and diverse chemical composition of real wastewater, which contains a variety of toxic metals and exhibits dynamic characteristics.

Acknowledgments

"This project was funded by the National Plan for Science, Technology and Innovation (MAARIFAH), King Abdulaziz City for Science and Technology, Kingdom of Saudi Arabia, Award Number (11-WAT1875-02)".

Conflict of Interest

Authors declare no conflict of interest.

References

Abia A.A., Horsfall M.J. and Didi O. (2002), Studies on the use of agricultural by-product for the removal of trace metals from aqueous solutions, *Journal of Applied Sciences and Environmental Management*, **6**(2), 89–95,

Ahmad A.A. and Hameed B.H. (2010), Fixed-bed adsorption of reactive azo dye onto granular activated carbon prepared from waste, *Journal of Hazardous Materials*, **175**(1–3), 298–303.

Aksu Z. (2005), Application of biosorption for the removal of organic pollutants: a review, *Process Biochemistry*, **40**(3–4), 997–1026,

Aksu Z. and Gönen F. (2004), Biosorption of phenol by immobilized activated sludge in a continuous packed bed: prediction of breakthrough curves, *Process Biochemistry*, **39**(5), 599–613,

Ali I., Al-Othman Z.A., Alwarthan A., Asim M., and Khan T.A. (2014), Removal of arsenic species from water by batch and column operations on bagasse fly ash, *Environmental Science and Pollution Research International*, **21**(5), 3218–3229,

Amin M.T., Alazba A.A. and Shafiq M. (2016), Adsorption of copper (Cu^{2+}) from aqueous solution using date palm trunk fibre: isotherms and kinetics, *Desalination and Water Treatment*, **57**(47), 22454–22466,

Amuda O., Amoo I., and Ajayi O. (2006), Performance optimization of coagulant/flocculant in the treatment of wastewater from a beverage industry, *Journal of Hazardous Materials*, **129**(1-3), 69–72.

Annadurai G., Juang R.S. and Lee D.J. (2003), Adsorption of heavy metals from water using banana and orange peels, *Water Science & Technology*, **47**(1), 185–190,

Apiratikul R. and Pavasant P. (2008), Batch and column studies of biosorption of heavy metals by Caulerpa lentillifera, *Bioresource Technology*, **99**(8), 2766–2777,

Areco M.M. and Afonso M. dos S. (2010), Copper, zinc, cadmium and lead biosorption by Gymnogongrus torulosus. Thermodynamics and kinetics studies, *Colloids and Surfaces B: Biointerfaces*, **81**(2), 620–628.

Aydin H., Bulut Y. and Yerlikaya Ç. (2008), Removal of copper (II) from aqueous solution by adsorption onto low-cost adsorbents, *Journal of Environmental Management*, **87**(1), 37–45.

Barakat M.A. (2011), New trends in removing heavy metals from industrial wastewater, *Arabian Journal of Chemistry*, **4**(4), 361–377.

Baral S.S., Das N., Ramulu T.S., Sahoo S.K., Das S.N. and Chaudhury G.R. (2009), Removal of Cr(VI) by thermally activated weed

Salvinia cucullata in a fixed-bed column, *Journal of Hazardous Materials*, **161**(2–3), 1427–1435.

Bhaumik M., Setshedi K., Maity A. and Onyango M.S. (2013), Chromium(VI) removal from water using fixed bed column of polypyrrole/Fe_3O_4 nanocomposite, *Separation and Purification Technology*, **110**, 11–19.

Blöcher C., Dorda J., Mavrov V., Chmiel H., Lazaridis N.K. and Matis K.A. (2003), Hybrid flotation—membrane filtration process for the removal of heavy metal ions from wastewater, *Water Research*, **37**(16), 4018–4026.

Boudrahem F., Aissani-Benissad F. and Soualah A. (2011), Adsorption of Lead(II) from Aqueous Solution by Using Leaves of Date Trees as an Adsorbent, *Journal of Chemical & Engineering Data*, **56**(5), 1804–1812.

Bulut Y. and Tez Z. (2007), Adsorption studies on ground shells of hazelnut and almond, *Journal of Hazardous Materials*, **149**(1), 35–41.

Chary N.S., Kamala C.T. and Samuel Suman Raj D. (2008), Assessing risk of heavy metals from consuming food grown on sewage irrigated soils and food chain transfer, *Ecotoxicology and Environmental Safety*, **69**(3), 513–524.

Cheraghi E., Ameri E. and Moheb A. (2016), Continuous biosorption of Cd(II) ions from aqueous solutions by sesame waste: thermodynamics and fixed-bed column studies, *Desalination and Water Treatment*, **57**(15), 6936–6949.

Chieng H.I., Lim L.B.L. and Priyantha N. (2015), Enhancing adsorption capacity of toxic malachite green dye through chemically modified breadnut peel: equilibrium, thermodynamics, kinetics and regeneration studies, *Environmental Technology*, **36**(1), 86–97.

Dąbrowski A., Hubicki Z., Podkościelny P. and Robens E. (2004), Selective removal of the heavy metal ions from waters and industrial wastewaters by ion-exchange method, *Chemosphere*, **56**(2), 91–106.

Djeribi R. and Hamdaoui O. (2008), Sorption of copper(II) from aqueous solutions by cedar sawdust and crushed brick, *Desalination*, **225**(1–3), 95–112.

El Nemr A., Khaled A., Abdelwahab O. and El-Sikaily A. (2008), Treatment of wastewater containing toxic chromium using new activated carbon developed from date palm seed, *Journal of Hazardous Materials*, **152**(1), 263–275.

El-Bindary A.A., Hussien M.A., Diab M.A. and Eessa A. M. (2014), Adsorption of Acid Yellow 99 by polyacrylonitrile/activated carbon composite: Kinetics, thermodynamics and isotherm studies, *Journal of Molecular Liquids*, **197**, 236–242.

El-Kamash A.M. (2008), Evaluation of zeolite A for the sorptive removal of Cs+ and Sr2+ ions from aqueous solutions using batch and fixed bed column operations, *Journal of Hazardous Materials*, **151**(2-3), 432–445.

Ertaş R. and Öztürk N. (2013), Removal of lead from aqueous solutions by using chestnut shell as an adsorbent, *Desalination and Water Treatment*, **51**(13-15), 2903–2908.

Futalan C.M., Kan C.-C., Dalida M.L., Pascua C. and Wan M.-W. (2011), Fixed-bed column studies on the removal of copper using chitosan immobilized on bentonite, *Carbohydrate Polymers*, **83**(2), 697–704.

Ghorbani F., Sanati A.M., Younesi H. and Ghoreyshi A.A. (2012), The potential of date-palm leaf ash as low-cost adsorbent for the removal of Pb(II) ion from aqueous solution, *International Journal of Engineering - Transactions B: Applications*, **25**(4), 269.

Al-Ghouti M.A., Li J., Salamh Y., Al-Laqtah N., Walker G. and Ahmad M.N.M. (2010), Adsorption mechanisms of removing heavy metals and dyes from aqueous solution using date pits solid adsorbent, *Journal of Hazardous Materials*, **176**(1–3), 510–520.

Goel J., Kadirvelu K., Rajagopal C. and Kumar Garg V. (2005), Removal of lead(II) by adsorption using treated granular activated carbon: Batch and column studies, *Journal of Hazardous Materials*, **125**(1–3), 211–220.

Guo J. and Lua A.C. (2003), Textural and chemical properties of adsorbent prepared from palm shell by phosphoric acid activation, *Materials Chemistry and Physics*, **80**(1), 114–119.

Gupta V.K., Ali I., Saleh T.A., Nayak A. and Agarwal S. (2012), Chemical treatment technologies for waste-water recycling—an overview, *RSC Advances*, **2**(16), 6380–6388.

Haleem A.M. and Abdulgafoor E.A. (2010), The Biosorption of Cr (VI) From Aqueous Solution Using Date Palm Fibers (Leef), *Al-Khwarizmi Engineering Journal*, **6**(4), 31–36.

Hamdaoui O. (2006), Dynamic sorption of methylene blue by cedar sawdust and crushed brick in fixed bed columns, *Journal of Hazardous Materials*, **138**(2), 293–303.

Han R., Wang Y., Yu W., Zou W., Shi J., and Liu H. (2007), Biosorption of methylene blue from aqueous solution by rice husk in a fixed-bed column, *Journal of Hazardous Materials*, **141**(3), 713–718.

Han R., Wang Yu, Zhao X., Wang Yuanfeng, Xie F., Cheng J. and Tang M. (2009), Adsorption of methylene blue by phoenix tree leaf powder in a fixed-bed column: experiments and prediction of breakthrough curves, *Desalination*, **245**(1–3), 284–297.

Han R., Zhang J., Zou W., Xiao H., Shi J. and Liu H. (2006), Biosorption of copper(II) and lead(II) from aqueous solution by chaff in a fixed-bed column, *Journal of Hazardous Materials*, **133**(1–3), 262–268.

Hikmat N.A., Qassim B.B., Khethi M.T., Hikmat N.A., Qassim B.B. and Khethi M.T. (2014), Thermodynamic and Kinetic Studies of Lead Adsorption from Aquesous Solution onto Petiole and Fiber of Palm Tree, *American Journal of Chemistry*, **4**(4), 116–124.

Hilal N.M., Ahmed I.A. and El-Sayed R.E. (2012), Activated and Nonactivated Date Pits Adsorbents for the Removal of Copper(II) and Cadmium(II) from Aqueous Solutions, *International Scholarly Research Notices*, **2012**, e985853.

Ho Y.S., Porter J.F. and McKay G. (2002), Equilibrium Isotherm Studies for the Sorption of Divalent Metal Ions onto Peat: Copper, Nickel and Lead Single Component Systems, *Water, Air, and Soil Pollution*, **141**(1-4), 1–33.

Hutchins R.A. (1973), New method simplifies design of activated-carbon systems [Reprod.], *Chemical engineering*, **80**, 133–138.

Jiménez-Cedillo M.J., Olguín M.T., Fall C. and Colin-Cruz A. (2013), As(III) and As(V) sorption on iron-modified non-pyrolyzed and pyrolyzed biomass from Petroselinum crispum (parsley), *Journal of Environmental Management*, **117**, 242–252.

Kapur M. and Mondal M.K. (2016), Design and model parameters estimation for fixed–bed column adsorption of Cu(II) and Ni(II) ions using magnetized saw dust, *Desalination and Water Treatment*, **57**(26), 12192–12203.

Khan M.S.M. and Kaneesamkandi Z. (2013), Biodegradable waste to biogas: Renewable energy option for the Kingdom of Saudi Arabia, *International Journal of Innovation and Applied Studies*, **4**(1), 101–113.

Khitous M., Moussous S., Selatnia A. and Kherat M. (2016), Biosorption of Cd(II) by Pleurotus mutilus biomass in fixed-bed column: experimental and breakthrough curves analysis, *Desalination and Water Treatment*, **57**(35), 16559–16570.

Khosa M.A., Wu J. and Ullah A. (2013), Chemical modification, characterization, and application of chicken feathers as novel biosorbents, *RSC Advances*, **3**(43), 20800–20810.

Ko D.C.K., Porter J.F. and McKay G. (2000), Optimised correlations for the fixed-bed adsorption of metal ions on bone char, *Chemical Engineering Science*, **55**(23), 5819–5829.

Lee V.K.C., Porter J.F. and McKay G. (2001), Modified Design Model for the Adsorption of Dye onto Peat, *Food and Bioproducts Processing*, **79**(1), 21–26.

Malkoc E., Nuhoglu Y. and Dundar M. (2006), Adsorption of chromium(VI) on pomace—An olive oil industry waste: Batch and column studies, *Journal of Hazardous Materials*, **138**(1), 142–151.

Mavrov V., Stamenov S., Todorova E., Chmiel H. and Erwe T. (2006), New hybrid electrocoagulation membrane process for removing selenium from industrial wastewater, *Desalination*, **201**(1-3), 290–296.

Mohan D. and Pittman C.U. (2007), Arsenic removal from water/wastewater using adsorbents—A critical review, *Journal of Hazardous Materials*, **142**(1-2), 1–53.

Momcilovic M., Purenovic M., Bojic A., Zarubica A. and Ranđelovic M. (2011), Removal of lead(II) ions from aqueous solutions by adsorption onto pine cone activated carbon, *Desalination*, **276**(1-3), 53–59.

Olgun A., Atar N. and Wang S. (2013), Batch and column studies of phosphate and nitrate adsorption on waste solids containing boron impurity, *Chemical Engineering Journal*, **222**, 108–119.

Oller I., Malato S. and Sánchez-Pérez J.A. (2011), Combination of Advanced Oxidation Processes and biological treatments for wastewater decontamination—A review, *Science of The Total Environment*, **409**(20), 4141–4166.

Osman H.E., Badwy R.K. and Ahmad H.F. (2010), Usage of some agricultural by-products in the removal of some heavy metals from industrial wastewater, *Journal of Phytology*, **2**(3), 51–62.

Pilli S.R., Goud V.V. and Mohanty K. (2012), Biosorption of Cr(VI) on immobilized Hydrilla verticillata in a continuous up-flow packed bed: prediction of kinetic parameters and breakthrough curves, *Desalination and Water Treatment*, **50**(1-3), 115–124.

Qadeer R. and Akhtar S. (2005), Kinetics study of lead ion adsorption on active carbon, *Turkish Journal of Chemistry*, **29**(1), 95–100.

Rajamohan N., Rajasimman M. and Dilipkumar M. (2014), Parametric and kinetic studies on biosorption of mercury using modified Phoenix dactylifera biomass, *Journal of the Taiwan Institute of Chemical Engineers*, **45**(5), 2622–2627.

Rao K.S., Anand S. and Venkateswarlu P. (2011), Modeling the kinetics of Cd(II) adsorption on Syzygium cumini L leaf powder in a fixed bed mini column, *Journal of Industrial and Engineering Chemistry*, **17**(2), 174–181.

Riaz M., Nadeem R., Hanif M.A., Ansari T.M. and Rehman K. (2009), Pb(II) biosorption from hazardous aqueous streams using Gossypium hirsutum (Cotton) waste biomass, *Journal of Hazardous Materials*, **161**(1), 88–94.

Sadaf S. and Bhatti H.N. (2014), Evaluation of peanut husk as a novel, low cost biosorbent for the removal of Indosol Orange RSN dye from aqueous solutions: batch and fixed bed studies, *Clean Technologies and Environmental Policy*, **16**(3), 527–544.

Sadaf S., Bhatti H.N., Nausheen S. and Amin M. (2015), Application of a novel lignocellulosic biomaterial for the removal of Direct Yellow 50 dye from aqueous solution: Batch and column study, *Journal of the Taiwan Institute of Chemical Engineers*, **47**, 160–170.

Sajab M.S., Chia C.H., Zakaria S. and Sillanpää M. (2015), Fixed-bed column studies for the removal of cationic and anionic dyes by chemically modified oil palm empty fruit bunch fibers: single- and multi-solute systems, *Desalination and Water Treatment*, **55**(5), 1372–1379.

Saka C., Şahin Ö. and Küçük M.M. (2012), Applications on agricultural and forest waste adsorbents for the removal of lead (II) from contaminated waters, *International Journal of Environmental Science and Technology*, **9**(2), 379–394.

Santhy K. and Selvapathy P. (2006), Removal of reactive dyes from wastewater by adsorption on coir pith activated carbon, *Bioresource Technology*, **97**(11), 1329–1336.

Sari A., Tuzen M., Uluözlü Ö.D. and Soylak M. (2007), Biosorption of Pb(II) and Ni(II) from aqueous solution by lichen (Cladonia furcata) biomass, *Biochemical Engineering Journal*, **37**(2), 151–158.

Sciban M., Radetic B., Kevresan Z. and Klasnja M. (2007), Adsorption of heavy metals from electroplating wastewater by wood sawdust, *Bioresource Technology*, **98**(2), 402–409.

Singh R., Gautam N., Mishra A. and Gupta R. (2011), Heavy metals and living systems: An overview, *Indian Journal of Pharmacology*, **43**(3), 246–253.

Soliman A.M., Elwy H.M., Thiemann T., Majedi Y., Labata F.T. and Al-Rawashdeh N.A.F. (2016), Removal of Pb(II) ions from aqueous solutions by sulphuric acid-treated palm tree leaves, *Journal of the Taiwan Institute of Chemical Engineers*, **58**, 264–273.

Song C., Wu S., Cheng M., Tao P., Shao M. and Gao G. (2013), Adsorption Studies of Coconut Shell Carbons Prepared by KOH Activation for Removal of Lead(II) From Aqueous Solutions, *Sustainability*, **6**(1), 86–98.

Sternberg S.P.K. and Dorn R.W. (2002), Cadmium removal using Cladophora in batch, semi-batch and flow reactors, *Bioresource Technology*, **81**(3), 249–255.

Tan W.T. (1985), Copper (II) adsorption by waste tea leaves and coffee powder, *Pertanika*, **8**(2), 223–230.

Teng M.-Y. and Lin S.-H. (2006), Removal of basic dye from water onto pristine and HCl-activated montmorillonite in fixed beds, *Desalination*, **194**(1–3), 156–165.

Thomas H.C. (1944), Heterogeneous Ion Exchange in a Flowing System, *Journal of the American Chemical Society*, **66**(10), 1664–1666.

Titi O.A. and Bello O.S. (2015), An Overview of Low Cost Adsorbents for Copper (II) Ions Removal, *Journal of Biotechnology & Biomaterials*, **5**(1), 1–13.

Uzunoğlu D., Gürel N., Özkaya N. and Özer A. (2014), The single batch biosorption of copper(II) ions on Sargassum acinarum, *Desalination and Water Treatment*, **52**(7-9), 1514–1523.

Vázquez G., Alonso R., Freire S., González-Álvarez J. and Antorrena G. (2006), Uptake of phenol from aqueous solutions by adsorption in a Pinus pinaster bark packed bed, *Journal of Hazardous Materials*, **133**(1–3), 61–67.

Wong K.K., Lee C.K., Low K.S. and Haron M.J. (2003), Removal of Cu and Pb from electroplating wastewater using tartaric acid modified rice husk, *Process Biochemistry*, **39**(4), 437–445.

Yadav S.K., Singh D.K. and Sinha S. (2013), Adsorption study of lead(II) onto xanthated date palm trunk: kinetics, isotherm and mechanism, *Desalination and Water Treatment*, **51**(34-36), 6798–6807.

Yadav S.K., Sinha S. and Singh D.K. (2015), Chromium(VI) removal from aqueous solution and industrial wastewater by modified date palm trunk, *Environmental Progress & Sustainable Energy*, **34**(2), 452–460.

Yagub M.T., Sen T.K., Afroze S. and Ang H.M. (2015), Fixed-bed dynamic column adsorption study of methylene blue (MB) onto pine cone, *Desalination and Water Treatment*, **55**(4), 1026–1039.

Yoon Y.H. and Nelson J.H. (1984), Application of Gas Adsorption Kinetics I. A Theoretical Model for Respirator Cartridge Service Life, *American Industrial Hygiene Association Journal*, **45**(8), 509–516.

Zahra N. (2012), Lead removal from water by low cost adsorbents: a review, *Pakistan Journal of Analytical & Environmental Chemistry*, **13**(1), 01–08.

Zhu B., Fan T., and Zhang D. (2008), Adsorption of copper ions from aqueous solution by citric acid modified soybean straw, *Journal of Hazardous Materials*, **153**(1–2), 300–308.